Analysis of experimental data for ion-impact single ionization of helium with Monte Carlo event generators based on quantum theory

M. Dürr,[1] B. Najjari,[1] M. Schulz,[2] A. Dorn,[1] R. Moshammer,[1] A. B. Voitkiv,[1] and J. Ullrich[1]
[2]*Max-Planck-Institut für Kernphysik, Saupfercheckweg 1, 69117 Heidelberg, Germany*
[1]*University of Missouri-Rolla, Physics Department and LAMOR, Rolla, Missouri 65409, USA*
(Received 19 March 2007; published 15 June 2007)

Recent multiply differential experimental data taken with reaction microscopes severely challenge predictions of quantum mechanical few-body models. Here, we report on a thorough analysis of all known possible experimental resolution effects and their influence on the extracted cross sections. Using a Monte Carlo event generator to simulate true events on the basis of quantum calculations allows us to consistently incorporate all aspects of the experimental resolution of the reaction microscope. We study the effect of the instrumental function in single ionization of helium by 3.6 MeV/u Au^{53+} and 100 MeV/u C^{6+} ions and find it to significantly modify the simulated theoretical predictions. Nevertheless strong discrepancies between simulated and experimental data persist. Structures in the measured cross sections reported earlier, which could not be reproduced by theory, are thus not solely due to the experimental resolution. Our study suggests that the method using event generators, as routinely done in high-energy physics, provides the ultimate pathway of benchmarking calculations against experimental data on few-particle reactions studied with modern imaging techniques.

DOI: 10.1103/PhysRevA.75.062708 PACS number(s): 34.50.Fa, 07.05.Tp, 52.20.Hv

I. INTRODUCTION

The dynamics of strongly correlated few-body systems remains one of the unsolved and challenging problems in atomic physics. Single ionization of an atom by charged particle impact occurring in atomic collisions is a preferred subject of studies as it is the kinematically most complex among the one-electron processes. Ultimate insight into the collision dynamics is obtained by specifying the complete kinematical information of the final three-body continuum state, i.e., by recording so-called fully differential cross sections (FDCS). Such $(e,2e)$ data have been routinely measured for electron impact on atoms since the pioneering work of Ehrhardt *et al.* [1], and a rich body of FDCS has been generated in the literature. However, until recently the vast majority of the data was only available for severely restricted detection geometries, namely, essentially only for the electrons ejected into the scattering plane defined by the initial projectile momentum and the momentum transfer **q**, i.e., the difference between the initial and final projectile momentum. For relatively slow electron impact FDCS were also reported for electrons ejected outside the scattering plane [2–4], however, for fast electron impact such out-of-plane data became only available in 2006 [5].

Experiments studying electron impact single ionization using conventional techniques determine the collision kinematics from the momenta of the scattered projectile and the ejected electron. The recoil-ion momentum is then determined by momentum conservation. Considering single ionization by ion impact, the large projectile mass typically leads to a tiny deflection angle of the scattered projectile which ranges (depending on projectile mass and speed) from about 10^{-3} to 10^{-9} rad, which, at the low end, is far beyond the reach of any experimentally achievable resolution. Only for proton impact have FDCS been obtained by measuring the projectile momentum directly [6]. It was not until 1996, when the application of modern charged particle projection techniques in combination with a cold atomic target, so-called reaction microscopes, that ion-impact fragmentation experiments with full kinematical information of the collision became possible [7]. This was achieved by detecting the target fragments—the recoiling ion and one or more ejected electrons—in coincidence and thus determining the momentum of the undetected scattered projectile from momentum conservation. The first FDCS for ion-impact single ionization of helium were reported in 2001 [8]. In addition to being an experimental device capable of recording such data, a further outstanding feature of this imaging technique is the solid angle acceptance of essentially 4π for the final state fragments which allows covering a large fraction of the final-state momentum-phase space of the fragmentation channel under examination. Therefore electron emission after single ionization into all three spatial dimensions could be recorded yielding a complete three-dimensional (3D) image of the FDCS [9].

Then, surprisingly, not only quantitative but significant qualitative discrepancies between measured and calculated FDCS for 100 MeV/u C^{6+}+He singly ionizing collisions were reported out of plane [9]. For this kind of collision system corresponding to small perturbation parameters $\eta = Z_P/v_P$ (i.e., the projectile charge to velocity ratio in atomic units with $e=\hbar=m_e=1$) the Born approximation (FBA) was thought to provide an adequate description of the ionization process. The features in the FDCS as a function of the electron ejection angle predicted by the FBA, in turn, are relatively simple: the scattering plane is characterized by the well known binary-recoil double lobe structure and in the plane perpendicular to **q** the angular dependence is isotropic. Furthermore, the FDCS follow a simple η^2 scaling so that for equal η the angular dependencies of the cross sections for electron and ion impact are identical. As for electron impact, the data for 100 MeV/u C^{6+}+He (η=0.1 a.u.) in the scatter-

 ©2007 The American Physical Society

ing plane were in good agreement with the FBA (except for very large q) [10], but outside the scattering plane even more sophisticated calculations (e.g., using distorted waves) were not able to reproduce the measured FDCS [9,11]. These results sparked significant research activity to understand these discrepancies, both experimental [5,6,12–16] and theoretical [10,17–21] and, similar features for out-of-plane electron ejection were recently reported for electron impact ionization of He [5,12] and of Mg [13] as well. In all cases the experimental results were interpreted in terms of a higher-order ionization process involving additional elastic scattering of the projectile by the residual target core. For the Mg data the origin of the out-of-plane features was confirmed by various theoretical models [13,18], and arguments were provided why theory is incapable of reproducing the same features for the case of ion impact [18].

Another collision system attracting considerable attention is single ionization of helium by medium velocity (v_P = 12 a.u.) Au^{53+} ions. Because of the unusually large perturbation of η=4.4 a.u. this collision system represents an extreme manifestation of the difficulties associated with the three-body Coulomb problem. Theoretically, sophisticated models have been developed over the past decades using continuum distorted waves (CDW) or the symmetric Eikonal approximation (SEA) which even at highest perturbations correctly predict total ionization cross sections and multiply differential cross sections as a function of ejected electron parameters. However, whenever cross sections differential in the projectile-momentum transfer to the target were analyzed, uncovering unprecedented details of the collision dynamics, all state-of-the-art quantum models failed. The interaction between the projectile and the target nucleus was proven to be of vital importance to understand the collision process, as was demonstrated for doubly differential cross sections presented as a function of momentum transfer [14]. For fully differential cross sections at these large perturbations, the electron emission pattern exhibits a strong peak in the direction of the outgoing projectile and actually becomes the dominant feature [16]. In the last five years various theoretical models were developed to explain the peak structures, especially for ion impact (e.g., Refs. [22–25]). However, none of these models up to the present day could reproduce the experimental structures even qualitatively.

Recently, it was claimed in a series of publications that the observed discrepancies are merely a result of the experimental resolution, which was assumed to be dominated by the finite temperature of the atomic target beam [19–21]. For single ionization of helium by 3.6 MeV/u Au^{53+} ions these authors showed that a target temperature of 16 K, about one order of magnitude larger than the reported experimental value, was required for the convoluted theory to at least partially reproduce the data [19]. For 100 MeV/u C^{6+} collisions, a convoluted continuum distorted wave (CDW) calculation assuming a temperature of 1 K was presented, where the authors claim that the observed out-of-plane structures are entirely due to the experimental resolution [21].

That there are effects, and that these effects can indeed be significant, has been well-known since early papers of Ullrich *et al.* [26] and Dörner *et al.* [27], where the results from classical trajectory Monte Carlo calculations by Olson had to be convoluted with the temperature in order to reproduce the then emerging results for recoil-ion momentum spectra. Therefore in all papers the target temperature was stated such that theory in principle should be able to include the experimental resolution. In practice this was often not possible since elaborate theoretical calculations lasted days or even months to generate one particular FDCS under a given geometry. In some cases at least a few calculations where performed within the experimental acceptance in order to estimate effects of the resolution.

Here, we present a systematic and thorough analysis of the effects of the experimental resolution on the measured differential cross sections. We report on the first complete—to the best of our knowledge—simulation of the image function on multiply differential data for single ionization of helium by 3.6 MeV/u Au^{53+}, 100 MeV/u C^{6+} ion impact. This was achieved by developing a quantum-theory-based Monte Carlo event generator. In contrast to the work of Olson and collaborators, who only accounted for the resolution due to the target temperature [19–21], we include all known contributions to the overall resolution as, e.g., the finite size of the interaction volume, finite time, and position resolutions of the detectors for ions and electrons, etc. Moreover, for the case of 1 keV electron impact we report two different measurements with different resolutions in order to experimentally evaluate its effect independently of theoretical modeling.

We confirm that the experimental resolution has an effect on the shape and absolute magnitude of the cross sections as expected and in principle known previously. We also unambiguously prove that the resolutions and temperatures stated in all our previous papers are correct within a factor of at most 2 and are in strong disagreement with the assumptions of Olson *et al.* [19]. Furthermore, we demonstrate that the momentum profile of our target beam is predominantly thermal and does not have any non-Gaussian large-momentum wings on a level of 10^{-2} relative intensity, in contrast to what was implied by Olson *et al.* [19]. Most importantly, indisputable and strong discrepancies between theory and experiment persist for the large perturbation, even when the calculations are convoluted with a resolution which is unrealistically low. For the perturbative situation, i.e., for 100 MeV/u carbon impact, the situation is more delicate and for small q the event-generator simulated data come closer to the experimental out-of-plane values. However, even in this case discrepancies remain and cannot be consistently traced back to result exclusively from the experimental image function. Furthermore, while in the calculation for large q the convolution with the resolution has essentially no effect at all qualitative discrepancies to the experimental data persist. Finally, comparison at this small η to our electron impact data reveals further conflicts with the convoluted calculations. More importantly, at large q the convoluted theory does not even reproduce the data qualitatively. The qualitative features in the experimental FDCS are thus not solely due to an artifact of the experimental resolution. Our present results clearly demonstrate that reaction microscopes are generally well suited for FDCS measurements and that valuable information can be extracted if, as is the case for any experimental data, the resolution is thoroughly accounted for in the comparison with theory.

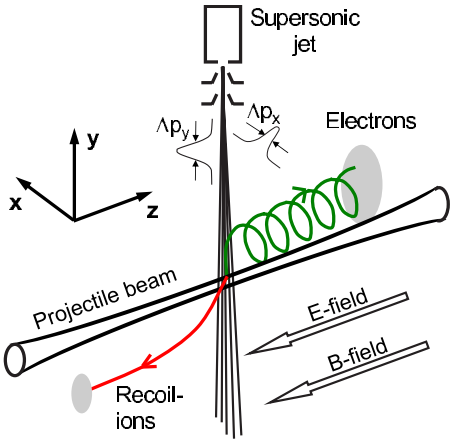

FIG. 1. (Color online) Schematic view of the reaction microscope.

II. THE REACTION MICROSCOPE

In the following section we present a thorough analysis of the experimental resolution of the reaction microscope. We first provide a brief description of the experimental setup followed by a discussion of the momentum resolution achieved for the recoil-ion and electron momentum vectors. A model of the instrumental function is implemented in a Monte Carlo–type of simulation using single ionization events generated according to predictions of quantum mechanical theoretical models. More technical details on reaction microscopes can be found in several review articles [7,28,29] or in Ref. [30].

A. Operation principle of reaction microscopes

The operation principle of the reaction microscope and specific geometrical settings used for kinematically complete experiments in charged particle collisions is illustrated in Fig. 1 and are briefly outlined here: A beam of fast ions crosses a cold beam of target atoms emerging from a supersonic gas jet. The target fragments produced by ionization in the interaction volume, i.e., the recoiling ion and one (or more) ejected electrons are extracted by a weak uniform electric field $E_{\|}$ in opposite directions. The electric field is directed parallel to the incoming beam direction along the z axis and is generated over a distance of $a=11$ cm with an acceleration voltage U. After acceleration, both the electron and the recoil ion traverse a field free drift region of $d=22$ cm. After passing through the drift region the charged particles are detected by two time and position sensitive large-area detectors (40 and 80 mm in diameter). Since fairly small extraction fields have to be applied (a few V/cm) to achieve high momentum resolution, a uniform magnetic field aligned along the extraction field is required in order to enhance the detection efficiency for electrons emitted transverse to the extraction field. Because of the ions larger mass the magnetic field only has a minor effect on their trajectories. The motion of the electrons, in contrast, is strongly affected with the magnetic field forcing them onto several cyclotron turns before reaching the detector.

From the arrival times and positions, the momenta of the target fragments are reconstructed in the offline analysis by tracing back their trajectories to the intersection point. We use the following Cartesian coordinate system: The projectile beam-propagation, which is aligned along the electric extraction field, defines the z axis, the y direction is oriented along the target beam, and the x axis is transverse to both of them (Fig. 1). Regarding the collision dynamics, however, there is a cylindrical symmetry with respect to the projectile axis such that at times it is more convenient to express the momenta in cylindrical coordinates. Here we chose the convention of expressing the coordinates by $p_{\|}=p_z$ (longitudinal direction), $p_{\perp}=\sqrt{(p_x)^2+(p_y)^2}$ (transverse direction), and the azimuthal angle $\varphi=\arctan(p_y/p_x)$. The two component transverse vector is given by $\mathbf{p}_{\perp}=(p_x,p_y)=(p_{\perp},\varphi)$.

In our detection geometry the time-of-flight (TOF) yields information on the longitudinal and the position on the detector on the transverse momentum component $p_{\|}$ and $\mathbf{p}_{\perp}$. The time-of-flight t_0 for a charged particle created at the interaction volume at rest to reach the detector can be easily calculated solving the Newtonian equations of motion and yields $t_0=(2a+d)\sqrt{M/(2qU)}$ (M: mass, q: charge state). For typical extraction fields (1–5 V/cm) t_0 for an ion is in the range of a few microseconds, whereas the lighter electrons only need a few hundred nanoseconds to reach the detector. For a fragment generated with nonzero momentum the TOF is altered with respect to t_0 (typically by up to a few tens of nanoseconds), which allows us to reconstruct the longitudinal momentum component p_z. Since the drift path of the charged particles is twice as long as their acceleration path a Wiley-McLaren type of time focusing [31] is realized. Therefore, the time-of-flight of the charged particles becomes to first order independent of the initial starting position along the z direction, and is only determined by the initial momentum along that direction, thereby eliminating the effect of the finite size of the interaction volume. When the kinetic energy of the charged particle is much less than qU, which is the case for the recoil ions, a simple linear relation between its longitudinal momentum and the TOF is given by $p_{\|}=qU/a(t_0-t)$ [29]. If during the collision the recoil ion experiences a kick in the transverse direction, such that it obtains the momentum $\mathbf{p}_{\perp}$, the resulting velocity will lead to a displacement $\mathbf{r}_{\perp}=\mathbf{p}_{\perp}t_{\mathrm{ion}}/M$ with respect to ions with zero transverse momentum on the position sensitive detector. This relation is used to determine the transverse momentum components of the recoil ion from its position on the detector, where in good approximation t_{ion} can be set equal to t_0. At larger time-of-flight the displacement $r_{\perp}$ grows such that effects from the position resolution on the transverse momentum component of the ions depends on the TOF and thus on the applied extraction voltage.

For electrons, the extraction of the momentum components is somewhat more complicated because the energy of the ejected electron is much larger than that of the recoil ion (approximately by the mass ratio M_{ion}/m_e). As a result the TOF no longer depends linearly on the longitudinal momentum of the ejected electron. Nonetheless, the longitudinal momentum is still recovered from the TOF by means of an approximate, but very accurate, analytical function or by nu-

merical methods. While the electrons are accelerated and drift towards the electron detector, the magnetic field leads to a cyclotron motion in the xy plane, where the time of a full revolution is given by $T_{\mathrm{cyclotron}}=2\pi m_e/(eB)$. Note, that this time is equal for all electrons, regardless of their momenta. If the time-of-flight is an integer multiple of $T_{\mathrm{cyclotron}}$, all emitted electrons are focused to their initial starting point in the xy plane on the detector, which lies on the spectrometer axis. Under these particular conditions the focusing gives rise to nodal points in the electrons detector position and the transverse momentum acceptance becomes infinite (if there were no geometrical boundaries).

The momentum transferred from the projectile to the target, defined by $\mathbf{q}=\mathbf{p}_0-\mathbf{p}_1$ ($\mathbf{p}_0$, $\mathbf{p}_1$: incoming and scattered projectile momentum, respectively), is deduced from the target fragment momenta by $\mathbf{q}=\mathbf{k}+\mathbf{p}_{\mathrm{rec}}$ exploiting momentum conservation, where $\mathbf{k}$ denotes the electron momentum and $\mathbf{p}_{\mathrm{rec}}$ the recoil-ion momentum.

B. Recoil-ion and electron momentum resolution

A main prerequisite for kinematically complete investigations using reaction microscopes involving recoil-ion detection is that the momentum resulting from the thermal motion in the target is small compared to the change in momentum a target atom experiences during the collision. Therefore a cold target needs to be prepared where in most spectrometers a beam of atoms cooled in an adiabatic supersonic expansion is used, which then allows for the determination of the collision kinematics with sufficient resolution without detection of the scattered projectile. For helium temperatures below 10 K are required in order to reduce the width of the momentum distribution from the thermal motion to less than 1 atomic unit. Thus, the initial momentum distribution of the target atoms characterized by the target temperature is one of the dominant factors for the experimentally achievable resolution of the ion-momentum in a reaction microscope experiment [before the reaction microscope was invented the ion spectroscopy alone was called the cold target recoil ion momentum spectroscopy (COLTRIMS)].

The details of the atomic beam source providing an internally cold target can be found in Refs. [7,29]. In the beam direction cooling is accomplished through adiabatic expansion of the target from high pressure (several atmospheres) to high vacuum (10^{-3} T). In the plane perpendicular to the expansion direction the beam is further cooled by collimation via a set of skimmers. The width of the thermal momentum distribution in the direction of the gas flow (y direction) is linked to the internal beam temperature by $\Delta p_y^{\mathrm{jet}} \approx 2.35\sqrt{Mk_bT}$ [full width at half maximum (FWHM)] [32]. For the specific design and pressure of our target jet the theoretical temperature for helium is less than 1 K corresponding to $\Delta p_y^{\mathrm{jet}} \leqslant 0.35$ a.u. FWHM. The theoretical width in the plane perpendicular to the expansion of about 0.12 a.u. FWHM due to skimming is considerably smaller.

Apart from the thermal motion of the target atoms, other contributions to the experimental resolution are present, for example the limited position and time resolution of the detection system. For the longitudinal direction the resolution of the ion TOF (less than 1 ns) can be safely neglected, as it contributes to the overall resolution only on a subpercent level. Due to the Wiley-McLaren time focusing the contribution of the finite reaction length along the z axis is negligible as well. As a result the inelasticity of the reaction can be extracted due to a superior resolution in the longitudinal direction. In the transverse direction, however, the position resolution may be significant. It contains two contributions, both affecting the transverse momentum components. First, the intrinsic detector resolution of the ion and electron detectors and second the finite size of the overlap between the projectile and target beams have to be taken into account. For the present setup the geometrical extension of the interaction volume is given by the size and shape of the projectile beam assuming that the projectile beam spot is smaller than the diameter of the atomic target beam.

For ions the spot size is directly mapped onto the position sensitive detector, which leads to a corresponding uncertainty in the determination of the recoil-ion transverse momentum. If for example the ionization event is displaced by δx from the ideal interaction point in the x direction, this leads to a mismatch $\delta p_x=\delta x M/t_{\mathrm{ion}}$ with respect to the true p_x for singly charged helium ions. A voltage of $U=50$ V and a displacement of $\delta x=1.0$ mm leads to an error of $\delta p_x=0.35$ a.u. The recoil ion detector employs a wedge and strip position encoding, where position resolutions of approximately 0.1 mm are achieved routinely. Therefore, in most cases the position resolution of the ions predominantly suffers from the finite size of the interaction volume. The effect can be reduced, at the expense of sacrificing transverse momentum acceptance, by extracting ions at lower voltages, which allows ions to spread over a larger transverse distance, and by a tight collimation of the projectile beam (values as small as 100 μm can be reached).

For electrons the relation between the inaccuracy in determining the position and the resulting uncertainty in momentum is not as straightforward, because of the complex electron motion. Furthermore, the timing resolution may play a role for the transverse components, since the number of traversed cyclotron turns needs to be known for reconstruction of the momenta. For an estimate we consider the error through the effective position resolution Δr which is a combination (error propagation of two Gaussian contributions) of the detector resolution and the finite beam size. Then, the resolution of the transverse momentum $k_\perp$ is given by $\Delta k_\perp=k_\perp \Delta r/r$, where r is the radial distance of the electron's detector position from the spectrometer axis [29]. For electrons with momentum $k_\perp=1$ a.u. hitting the detector at its outer rim at 40 mm, this leads to a momentum resolution of $\Delta k_\perp=0.025$ a.u. for $\Delta r=1$ mm. At flight times, which are integer multiples of the cyclotron revolution time, all electrons return to the axis ($r=0$) and no momentum resolution is achieved at all. In contrast, for TOFs which are in between such two nodes, the electrons have reached the point where they have the maximal distance r from the spectrometer axis and, hence, here the resolution of the transverse component is best. Therefore the value for $\Delta k_\perp$ stated above represents a lower limit. By cutting events where electrons are within the focusing node, which is done in the experimental data analysis, an upper limit can be established.

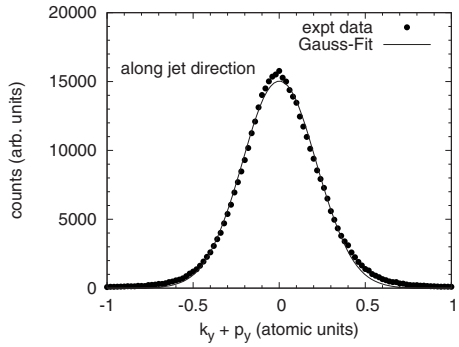

FIG. 2. (Top) The measured momentum resolution for the momentum components in direction of the atomic target beam after single ionization of He by an intense fs laser pulse. The solid curve represents a Gaussian fit, which gives a width of 0.5 a.u. (FWHM), corresponding to an internal jet-temperature of 2 K.

In summary, all of the contributions to the overall resolution discussed above add in a complicated manner, especially if highly differential data are extracted and/or if data are presented in terms of energy and angle rather than in terms of momenta. It is definitively impossible to unfold the experimental data and, thus, to remove effects due to the resolution. However, well-defined limits can certainly be (and always are) established as described above for the transverse and longitudinal momentum components of the electrons and the ions and those are usually stated in the respective experimental sections.

C. Determination of experimental parameters

After the main sources of the experimental resolution have been discussed, we present how we can experimentally determine upper limits for the various contributions to the instrumental function.

1. Thermal motion in the target beam along the jet direction

The achievable final temperature may critically depend on the actual conditions in the individual experiment. Here, we present evidence for the sufficient quality of the cooling mechanism via supersonic expansion. Using a reaction microscope with a very similar setup for preparation of the target beam, the momenta of the target fragments ionized by an intense femtosecond laser pulse [33] were measured. Since essentially no momentum is transferred by the light field, the sum momentum of the fragments has to equal zero. Therefore, the width of the experimentally obtained sum-momentum distribution in the respective directions reflects directly the overall resolution of the setup, which is shown in Fig. 2 for the components in the jet direction. An important advantage of ionizing with strong laser fields is the fact that ionization only takes place in the focus of the laser, which is less than 10 μm in the experiment. However, the recoil-ion position was measured using a delay-line anode, for which the position resolution is significantly worse (about 0.5 mm due to the time resolution of the multihit time-to-digital converter) than for a wedge and strip anode. Therefore, the measured width of the sum momentum distribution provides an upper limit for the temperature. A Gaussian fit of the sum momentum in the y direction yields a width of 0.5 a.u. (FWHM), which corresponds to a maximum internal beam temperature of 2 K. A slight deviation from a Gaussian distribution is observed at large sum momenta in the experiment, which can be explained by events where the electrons arrive at flight times where they are focused in a nodal point (i.e., where the electron momentum resolution is poor). Even if the increase in intensity at large momenta would be considered as contamination of the data by low resolution background, the contribution is in the percent level of the total number of events. This is indisputable proof, that "hot" components in the cooled atomic beam from a supersonic expansion represent a negligible contribution to the total number of recorded ionization events, if present at all. Our result clearly contradicts the speculation by Olson *et al.* [19], who suggested that hot components may lead to spurious contributions in the extraction of experimental cross sections using reaction microscopes. It is therefore clear that along the y direction the initial momentum distribution of the target beam is Gaussian and has a width of at most $\Delta p_y^{\text{jet}}=0.5$ a.u. FWHM. Taking the 0.5 mm position resolution in the present experiment approximately into account we arrive at $\Delta p_y^{\text{jet}}=0.35$ a.u. FWHM (corresponding to a temperature of about 1 K), exactly the number provided in most of the disputed papers.

2. Initial target-momentum distribution transverse to the jet flow

One might still argue that the experimental conditions in the ion-collision experiments might have been different from those with the femtosecond laser. Therefore, the momentum resolution of the helium atoms in the projectile-beam direction is directly obtained from the disputed experimental data for single ionization of helium. This is possible because in fast collisions the momentum transfer along the longitudinal direction is negligibly small (which is not the case in the direction transverse to the projectile beam so that there the laser data were needed). This negligibly small longitudinal momentum transfer can be explained by its relation to the projectile-energy loss ΔE through $q_z=k_z+p_z=\Delta E/v_P=(V_{\text{ion}}+E_e)/v_P$, where V_{ion} is the ionization potential and E_e the emitted electron energy. For swift ion-atom collisions the ejected electron energy distribution has its maximum at zero energy and rapidly drops at energies larger than about 5 to 10 eV (i.e., $E_e<1$ a.u.), while the projectile velocity reaches tens of atomic units. Hence, the electron energy can nearly be neglected (although it is usually extracted from the electron data) and, since V_{ion} is fixed, the width of the longitudinal momentum transfer spectrum is less than 0.05 atomic units, see, e.g., Ref. [34]. Along the longitudinal direction time focusing cancels the geometrical extension of the ionization volume and the momenta are gained from the time of flight, which ensures a superior resolution. Therefore the initial momentum spread of the target atoms Δp_z^{jet} is the dominant factor determining the final momentum resolution. A Gauss fit to the experimental spectrum for $q_z=k_z+p_z$, i.e., without correcting for the electron energy distribution, yields a width of 0.15 a.u. (FWHM), which is in accordance with the expected value for Δp_z^{jet}. It should be noted that the in-

ternal thermal momentum distribution in the jet is identical for both components perpendicular to the target beam direction, i.e., $\Delta p_x^{\mathrm{jet}} = \Delta p_z^{\mathrm{jet}} \leqslant 0.15$ a.u.

It should be mentioned, that the q_z spectrum is always monitored during the measurement. Apart from a constant factor q_z is reflected by the coincident sum TOF for the recoiling ion and the electron. Therefore, the coincidence time spectra, which are obviously essential to the experiment, readily provide the q_z spectrum.

3. Size of projectile and target beam overlap

Another experimental parameter, which can be reliably and directly estimated from the measured spectra is the overall position uncertainty of the electrons, which, as mentioned above, is a combination of the intrinsic detector resolution and the size of the spatial overlap of the projectile and the target beam in the xy plane, i.e., the size of the projectile beam focus at the location of the target beam. It can be directly deduced by analyzing the spot size of the electrons at flight times, at which all electrons are focused back to the spectrometer axis. From these spectra $\Delta x = 1$ mm is obtained, which we use as an upper limit for the projectile beam size in the ion-impact experiments discussed in this paper.

In summary, based on the considerations discussed above and assuming Gaussian error propagation, the individual contributions add to the overall momentum resolution of the recoiling ion leading to the following expressions

$$(\Delta p_x)^2 = (\Delta p_x^{\mathrm{jet}})^2 + (f\Delta x)^2$$

$$(\Delta p_y)^2 = (\Delta p_y^{\mathrm{jet}})^2 + (f\Delta y)^2$$

$$(\Delta p_z)^2 = (\Delta p_z^{\mathrm{jet}})^2,$$

with $f = \sqrt{M2qU}/(2a+d)$. We set $\Delta p_x^{\mathrm{jet}} = \Delta p_z^{\mathrm{jet}} = 0.15$ a.u. and $\Delta p_y^{\mathrm{jet}} = 0.5$ a.u., which are the upper limits for the widths of initial target-atom momentum distribution in the x, y, and z directions, and $\Delta x = 1$ mm, $\Delta y = 1$ mm are the upper limits for the overall resolution of the detector position in the respective direction. For electrons similar expressions for the resolution of the individual momentum components can be derived and were used in the following analysis, but are not explicitly stated here as the considerations are exactly identical and the contribution to the overall resolution is much smaller than that of the ions.

III. THE EVENT GENERATOR: IMPLEMENTING THE RESOLUTION INTO THEORY

In this section we present our method of folding the experimental resolution of the reaction microscope into "exact" theoretical cross sections, thus incorporating all aspects of the instrumental imaging function discussed in the previous section. For the three-body fragmentation, in principle folding over the five-dimensional final-state phase space has to be performed, which means that the cross sections have to be calculated for a large part of the final-state phase space. Such a procedure is prohibitively time consuming as theoretical models are numerically demanding. In addition, the complexity of the instrumental effects can make integration over convolution intervals unfeasible. Alternatively, the experimental effects on the various cross sections can be studied by generating an event file (similar to the experimental data file), consisting of a large number of ionization events, based on a theoretical calculation. For each ionization event the file contains five momentum components (which are required to fully determine the kinematics). This file thus represents a theoretical simulation of the events recorded during a measurement. From the simulated data, cross sections are extracted using the same analyzing procedure applied for the extraction of the real experimental spectra from the data. The experimental resolution can be modeled by adding (pseudo-)random numbers to the individual momentum components of each generated event, which simulate the various experimental uncertainties. The random numbers follow a certain distribution, which is chosen according to the expected instrumental influence, i.e., integrated over many events, the FWHM of the individual momentum-component spectra resemble the various effects due to the expected (and previously verified) uncertainty or upper limits thereof. The advantage of this method in terms of computational time is, that once the event file has been assembled, only the random numbers need to be generated, which is much less time consuming than the calculation of theoretical cross sections over the convolution range. This way the experimental error sources included in the simulation can be easily varied in order to systematically study their effect on the extracted cross sections.

In the present simulation each event is composed of the three momentum components of the ejected electron $\mathbf{k}$ and two components of the momentum transfer transverse to the incoming projectile beam $\mathbf{q}_\perp = (q_x, q_y)$. The collision kinematics is restricted to a range of $(0.1 \text{ a.u.} \leqslant |\mathbf{k}| \leqslant 2 \text{ a.u.}, |\mathbf{q}_\perp| \leqslant 2.2 \text{ a.u.})$, which corresponds to the typical acceptance of a reaction microscope experiment. The Monte Carlo generated events are selected using a simple rejection method, where the following cycle is repeatedly executed until a sufficiently large sample of "good" events has been generated.

(1) A set of six random numbers is chosen, five of which represent a point in the five-dimensional momentum phase space $(k_x, k_y, k_z, q_x, q_y)$ and are uniformly distributed within the limits stated above. The sixth random number u is uniformly distributed in the interval (0,1).

(2) The cross section is calculated at the randomly selected point $\sigma(k_x, k_y, k_z, q_x, q_y)$ from the theoretical model (in our case FBA or SEA). The random number u is compared with the normalized cross section $\tilde{\sigma}(k_x, k_y, k_z, q_x, q_y) = \sigma(k_x, k_y, k_z, q_x, q_y)/\sigma_{\max}$, where $\sigma_{\max}$ is the maximum of the cross section within the selected phase space, such that $\tilde{\sigma}$ ranges between zero and one. If $u < \tilde{\sigma}$ the five momenta are stored in the event file, but they are discarded if $u > \tilde{\sigma}$.

As the cross section drops rapidly towards larger electron momenta and momentum transfers, this method becomes quite inefficient, i.e., many events are rejected so that a lot of random numbers need to be generated until a sufficiently large event file was obtained. The efficiency of the rejection method can be significantly improved by modifying the weight of the randomly selected number u from a uniform to

another distribution, which is a better match to the cross section. Event files were produced for single ionization of helium by two different ionic projectiles. First, for 100 MeV/u C^{6+} ions with $v_P=60$ a.u., which is at a small perturbation parameter $Z_P/v_P=0.1$, one million events were generated using a first Born model. For this small perturbation the FBA yields essentially identical results to more sophisticated distorted wave type of calculations [10,21]. Second, an event file (580 000 events) for single ionization by 3.6 MeV/u Au^{53+} with $v_P=12$ a.u. ($Z_P/v_P=4.4$ a.u.) was produced. At this very large perturbation two theoretical models were used: the continuum distorted-wave–Eikonal initial state (EIS) and the symmetric Eikonal approximations (SEA). It was found that at small ejected electron velocities ($v_e \ll v_P$), which is satisfied in our case, both models yield essentially close results. Since our computer codes for the SEA model run faster than those of the CDW-EIS model and the generation of events turned out to be time-consuming, the simulated events were weighted according to the SEA model, where the details of the calculation dubbed "SEA-3HF-NN" can be found in Ref. [35]. The calculation is numerically far more demanding than the first Born model, so that a total time of 2 weeks using 40 CPU's in parallel was necessary to generate the ionization events at the large perturbation.

From the event files, differential cross sections are extracted exactly the same way as for the experimental data, i.e., by sorting event by event into a corresponding histogram. For example the FDCS is obtained by selecting events within particular ranges of momentum transfers, electron energies and by choosing events within the considered electron-emission plane (e.g., scattering plane) and plotting these events as a function of the polar electron ejection angle. As in the experimental data analysis the simulated differential cross sections are effectively integrated over the particular bin size and are thus treated on an equal footing as the experimental data. Since the underlying first Born and SEA model correctly predict the total single ionization cross sections with an accuracy of better than 10%, a comparison on an absolute scale is possible by normalizing the total number of generated events to measured total single ionization cross sections [36].

The next task is to implement the experimental resolution into the simulation. For each event, the transverse recoil momenta are determined from the given electron momentum and the momentum transfer. The initial momentum from the thermal motion in the target beam, the projectile beam size and the position and time resolution of the detectors are then included by generating random numbers $\delta p_z^{\mathrm{jet}}$, $\delta p_y^{\mathrm{jet}}$, δx, δy, $\delta x'$, $\delta y'$, and δt (where the unprimed position uncertainties represent the finite projectile beam size and the primed terms the intrinsic detector resolution) all individually distributed according to a Gaussian distribution centered at zero and with a width according to the respective uncertainty. In the case of the projectile-beam profile other distributions can be selected. For example, a rectangular profile would provide a realistic alternative description, since the ion beams where collimated by a pair of slits. Both shapes of the beam profile were tested in the simulation. Since the width of the beam profile is approximately equal in both x and y directions as inferred from the recorded electron spectra (see Sec. III C), we set $\Delta x=\Delta y$ in the simulations presented in this paper.

For the electrons the position uncertainty is included by first calculating the detector position (x_e,y_e) which is straightforwardly obtained from the full momentum vector $\mathbf{k}$. Then we add the random numbers δx, $\delta x'$ and δy, $\delta y'$ to x_e and y_e, respectively, and then recalculate the electron momentum, which is now inflicted with the error from the size of the interaction volume and from the intrinsic position resolution of the detector. The conversion from position back to momentum is a function of the time of flight, to which we add the random number δt. Because of the much better position resolution of the wedge and strip anode used on the recoil-ion detector, compared to the delay-line anode of the electron detector, its contribution to the overall experimental resolution is negligible. The convolution procedure was tested by first applying it to a δ function to ensure that the Monte Carlo procedure to generate the event file is free of errors. It should be noted that the recoil-ion momentum resolution due to the projectile beam size improves with decreasing extraction voltage U.

IV. COMPARISON OF CONVOLUTED THEORY WITH EXPERIMENT

With the simulation framework at hand we can now test the effect of any component of the experimental resolution on any type of differential cross section measured in the experiment. This is done by varying the random numbers, discussed in the previous section, which simulate the various contributions to the overall uncertainty in the convoluted calculation and comparing the result to the experimental data.

A. Single ionization of He by Au^{53+} ions

In Fig. 3 we show single differential cross sections as a function of the two components of the transverse momentum transfer q_x (top) and q_y (bottom) for 3.6 MeV/u Au^{53+}+He. The solid circles are the experimental data and the curves show the simulation for various beam size/temperature combinations. In the simulation of single ionization by Au^{53+} impact, the extraction voltage and the magnetic field were set to the values used in the experiment ($U=30$ V, $B=20$ G). The generated results have been scaled to the experimental data at the central peak maximum, since here only the width of the distribution is of interest. The measured spectrum in the x direction is roughly a factor 2–3 wider than the simulated unconvoluted spectrum (dashed curve labeled MC plain). The data in the y direction, which is the direction along the target beam, is clearly broader than in the x direction, which can easily be attributed to the poorer resolution resulting from the jet temperature.

A projectile beam size of 1 mm (solid curve in the top panel of Fig. 3) leads to a considerable broadening, however, the experimental width is only matched assuming a beam size of 1.5 mm (dotted curve). It should be noted that the upper limit of 1 mm (see Sec. III C) was determined for 100 MeV/u C^{6+}+He. For 3.6 MeV/u Au^{53+}+He the projectile beam was more tightly collimated so that even a beam

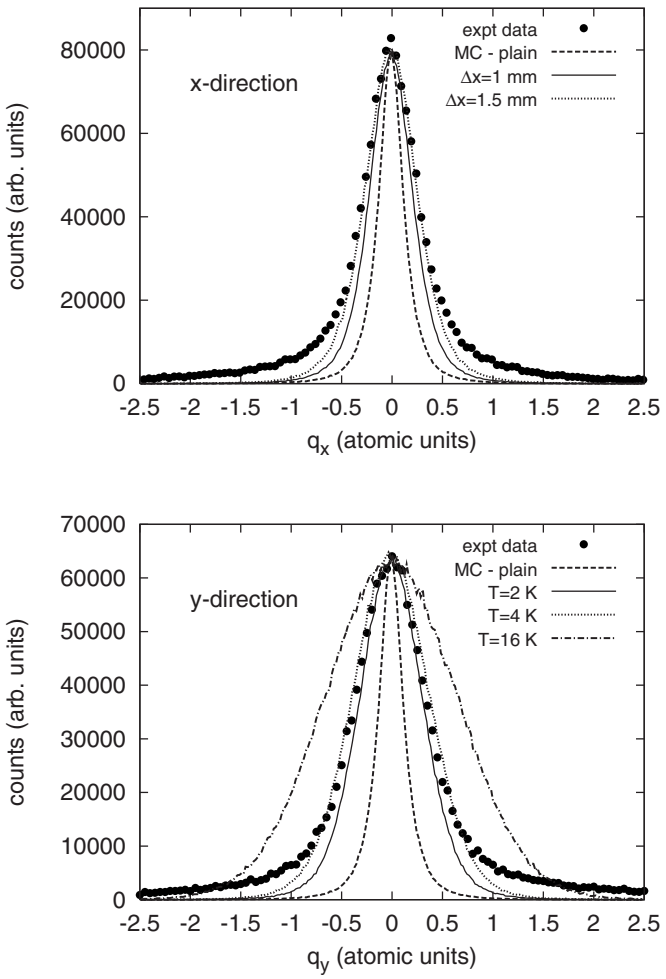

FIG. 3. Single differential cross sections for 3.6 MeV/u Au^{53+} single ionization of helium for the x (top) and y direction (bottom). Points: Experimental data, lines: Monte Carlo simulation results.

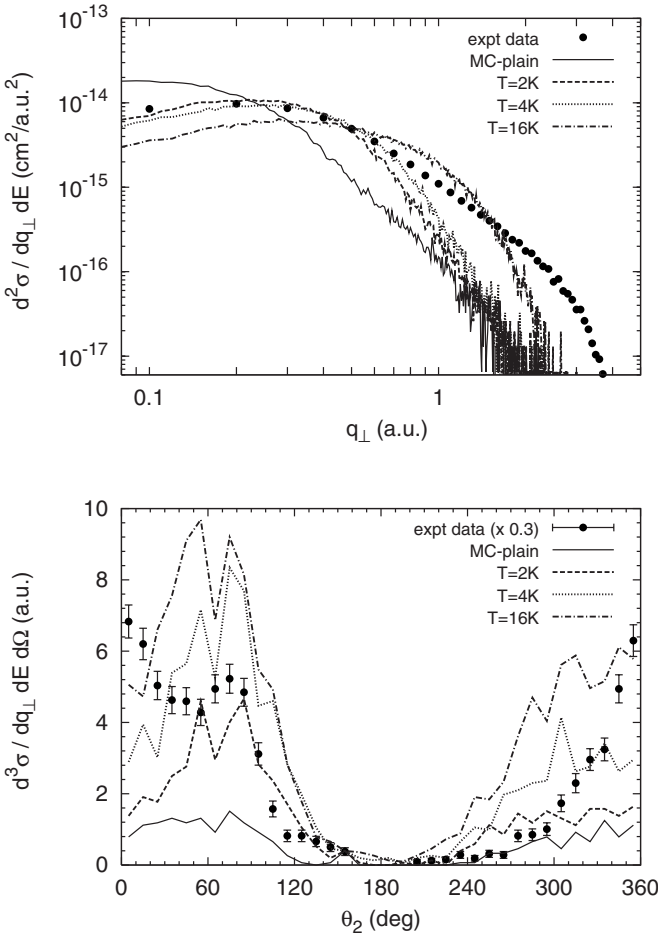

FIG. 4. Double differential (top) and fully differential cross sections (bottom) for single ionization of helium by 3.6 MeV/u Au^{53+} for an energy of the ejected electron $E_e=(10\pm3)$ eV. The FDCS is displayed in the scattering plane for a momentum transfer of $q_\perp=(1\pm0.3)$ a.u.

size of 1 mm is a significant overestimation. For the y direction (bottom panel of Fig. 3), the width is reproduced for a beam size of 1 mm and a target temperature of 2 K. A target beam temperature of 16 K (assumed by Olson *et al.* [19]) can clearly be ruled out, as it leads to a much broader distribution in the single differential cross section than observed experimentally (dash-dotted curve). This provides clear evidence that the data were obtained under clean experimental conditions with resolutions as stated in the original publication. In addition, it should be noted that for both the x and y directions the exact shape of the spectra is not reproducible regardless of which resolution is assumed in the simulation. This indicates that the SEA-3HF-NN model does not provide an adequate description of the collision process, in particular at increasing momentum transfers. Regardless of this model's deficiencies, the upper limits on the experimental uncertainties nevertheless remain valid, as they can be independently estimated from the width of the experimentally observed distribution.

It is certainly clear that the experimental resolution does affect the shape of the simulated spectra and, thus, of the measured spectra. We therefore extend the study of instrumental effects to higher differential projections, beginning with doubly differential cross sections $d\sigma/dq_\perp dE_e$ (DDCS). These DDCS plotted as a function of the transverse momentum transfer at fixed electron energy turned out to be an extremely sensitive test of perturbative calculations and have caused a lot of discussion [14]. In Fig. 4, we present simulated DDCS at an ejected electron energy of 10 eV (±3 eV), where the simulated results are compared with the experimental data [14] on an absolute scale. While the plain simulation result disagrees strongly with the experimental data for all $q_\perp$, the convoluted spectrum for a 1 mm × 1 mm projectile beam spot size and 2 K target temperature matches the experimental data very well at small momentum transfers. A similar effect of the resolution on the DDCS was estimated on simpler grounds but with nearly identical result in the original publication of the experimental data [14]. Strong discrepancies, however, persist at momentum transfers above approximately 0.7 a.u. even at an unrealistically large temperature of 16 K. In the region of large momentum transfers, the experimental data show strongly enhanced cross sections compared to the calculations.

Next, we analyze the FDCS, where the cross section is presented as a function of the polar electron emission angle

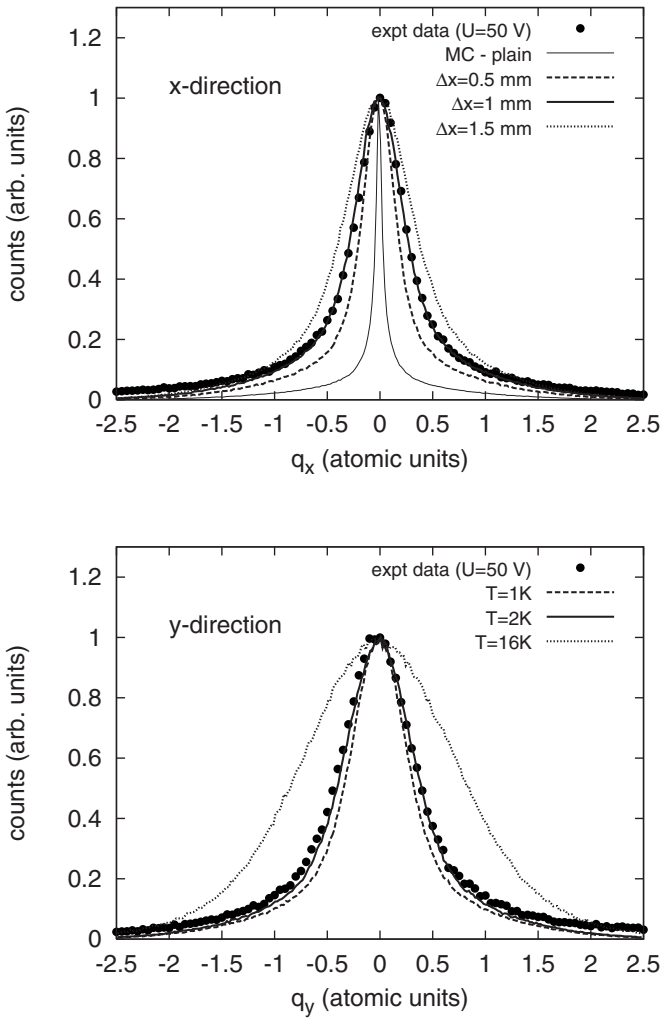

FIG. 5. Single differential cross sections for 100 MeV/u C^{6+} single ionization of helium for the x (top) and y direction (bottom). Points: Experimental data, lines: Monte Carlo simulation results.

at fixed electron energy and momentum transfer $q_\perp$. The events were binned over projectile momentum transfers $q_\perp$ =0.7 to 1.3 a.u. and electron energies E_e=7 to 13 eV. Ejected electron momenta within an azimuthal angle of ±10° with respect to the projectile-scattering plane are accepted. The absolute magnitude of the FDCS in Fig. 5 sensitively reacts to the target temperature, where the cross sections rises by a factor of 4 assuming a target temperature of T =2 K and in our worst scenario of T=16 K by a factor of 10. However, the shape of the cross section remains nearly unchanged in our simulation model. Comparing the simulation results with measured data strong discrepancies, both in shape and magnitude, prevail, in particular for the enhanced 0°-electron emission, which is the dominant peak in the experiment. It is thus clear that the calculation fails to reproduce the FDCS and that the forward peak is not just an artifact of the experimental resolution.

B. Single ionization of He by 100 MeV/u C^{6+} ions

As mentioned before, for 100 MeV/u C^{6+} collisions the FBA was used in the simulation, which is known to produce essentially identical results such as, e.g., the CDW-EIS model [10,21]. The measurement was performed at extraction voltages of U=50 V and 20 V and a magnetic field of B=20 G. Again, we start by analyzing the singly differential cross sections $d\sigma/dq_x$ and $d\sigma/dq_y$ with different simulated spot sizes of the projectile beam (Fig. 5). Almost perfect agreement is observed for a beam size of 1 mm (FWHM) in the x direction. In this particular experiment the overall ion-momentum resolution mostly suffers from the relatively large acceleration voltage, such that a beam profile of Δx =1 mm leads to an overall ion resolution (including the target temperature) of $\Delta p_{\mathrm{rec},x}$=0.4 a.u. The relatively large extraction voltage was chosen at will in order to guarantee acceptance for electrons at high energies thus covering a considerable part of the double-ionization final-state phase space, the original goal of that experiment. For the y direction the simulation is shown for a beam size of 1 mm and varying target temperatures T. The best fit is reached for a value of T=2 K, corresponding to an overall resolution in the y direction of $\Delta p_{\mathrm{rec},y}$=0.62 a.u. FWHM, which is consistent with the upper limit for the target temperature determined in the laser experiment (Fig. 2). It is interesting to note that at this lower perturbation the whole experimental spectrum up to relatively large momenta is now better reproduced indicating that the theoretical model is much more capable of describing the experimental data.

For the data taken with an extraction voltage of U =20 V all other experimental parameters, such as the profile of the projectile beam and the temperature of the target jet, remained the same. To further test the simulation model, we compare it with the data set at this lower extraction voltage. Since the size of the beam focus considerably contributes to the recoil-momentum resolution at higher extraction voltages, a major effect is expected in particular in the x direction, where this beam-size effect constitutes the dominant error source. For the low extraction voltage the simulation predicts an overall recoil-momentum resolution of $\Delta p_{\mathrm{rec},x}$ =0.27 a.u. and $\Delta p_{\mathrm{rec},y}$=0.55 a.u. As expected and illustrated in Fig. 6, the simulated SDCS $d\sigma/dq_x$ (but not $d\sigma/dq_y$) clearly reacts to the smaller extraction voltage. On the other hand the experimental data show nearly no effect. Hence there is an inconsistency between the simulation and experiment, where the simulation predicts a voltage dependent resolution which is not reflected in the data. One possibility for explaining this result might be an instrumental effect, which is independent of the extraction voltage that is responsible for the width of the spectrum of $d\sigma/dq_y$. The only candidate for such an error source is the electron momentum. An upper limit for the position resolution can be directly read from the electron position spectra. Even unrealistically large values for the position and time resolution cannot reproduce the observed spectra. Therefore, the inconsistencies in the effects of the extraction voltage on $d\sigma/dq_x$ between the simulation and the data are a first hint that the FBA has deficiencies in describing the collision dynamics. Furthermore, the insensitivity of the width in the experimental SDCS strongly suggest that the actual experimental parameters determining the resolution are significantly smaller than the upper limits used in the simulation, especially the projectile beam size.

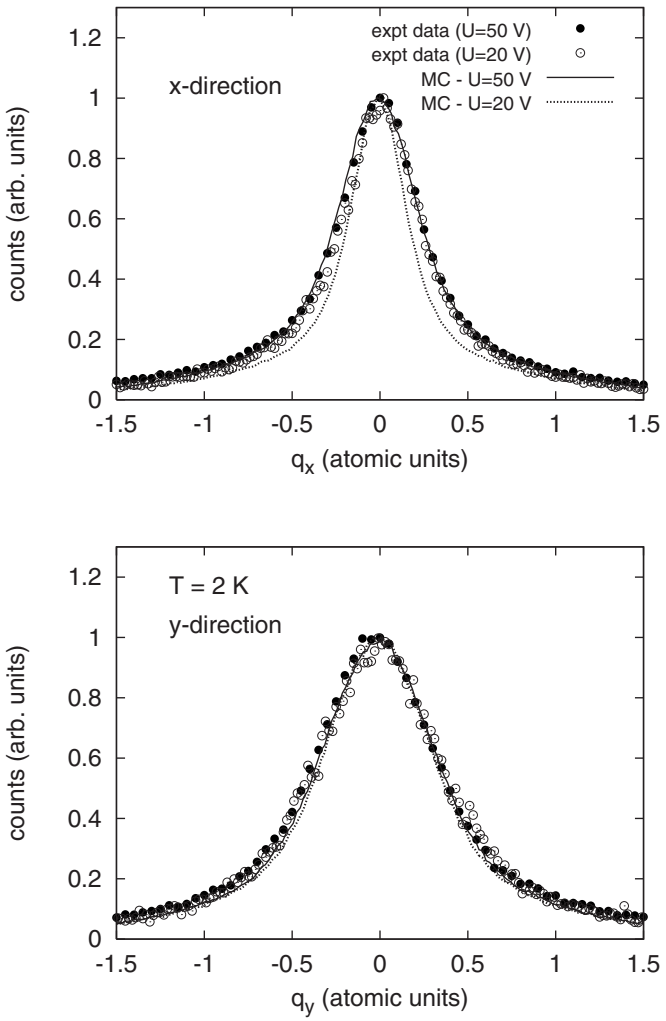

FIG. 6. Single differential cross sections for 100 MeV/u C^{6+} single ionization of helium for the x (top) and y direction (bottom). Lines: Monte Carlo simulation results with $\Delta x=\Delta y=1$ mm and $T=2$ K.

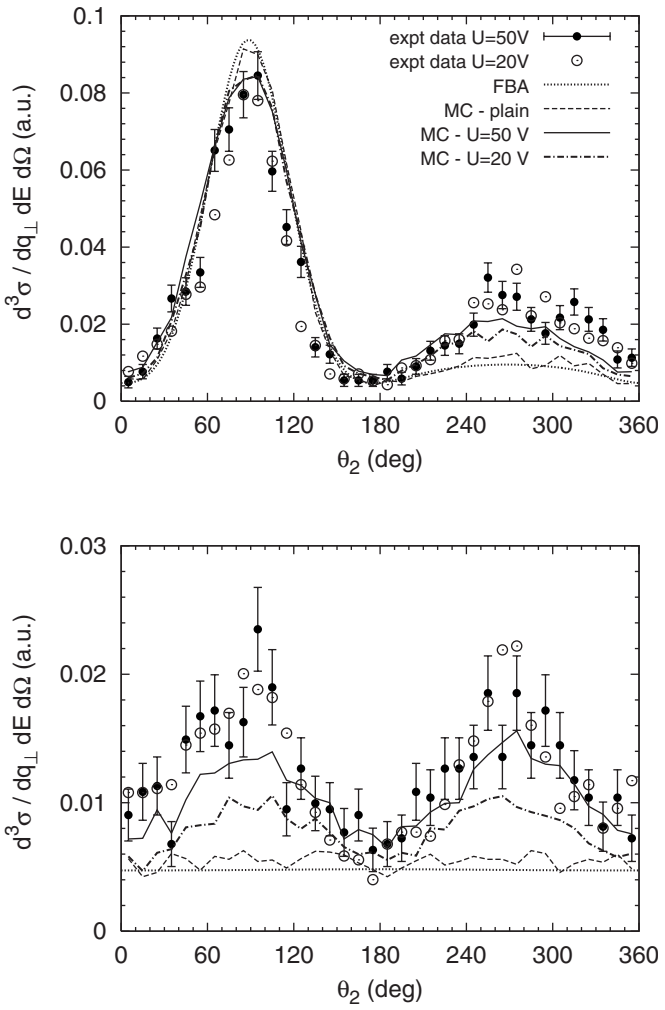

FIG. 7. Fully differential cross sections for single ionization of helium by 100 MeV C^{6+} in the scattering plane (top) and the plane perpendicular to the scattering plane (bottom). The energy of the ejected electron $E_e=(6.5\pm3.5)$ eV and the momentum transfer $q_\perp=(0.75\pm0.25)$ a.u. were chosen.

In Fig. 7 we show the FDCS for $E_e=(6.5\pm3.5)$ eV and $|\mathbf{q}|=(0.75\pm0.25)$ a.u. Two electron-emission planes were considered, the scattering plane and the plane perpendicular to the scattering plane and containing the projectile axis (here simply referred to as the "perpendicular plane"). Ejected electron momenta within an azimuthal angle of ±10° with respect to the selected plane are accepted. The FDCS extracted from the unconvoluted simulation (dashed curve) is compared with the "exact" FBA cross section (dotted curve), to study the influence of the finite size of the integration windows (Fig. 7). In the scattering plane the binary peak is not significantly affected by the momentum resolution whereas the recoil peak is more sensitive to the experimental resolution. Our simulation with $T=2$ K doubles the height of the recoil peak compared to the unconvoluted FBA results, but is still a factor 1.5 smaller than the peak height in the experimental data. A similar sensitivity of the FDCS to the resolution is observed for the perpendicular plane. Here, peak structures at 90° and 270° are produced in the simulation similar to those observed in the experimental data and absent in the unconvoluted FBA prediction, which is isotropic. It should be noted that convoluting the calculation only with the target temperature in the y direction of 1 K, as done by Fiol *et al.* [21], yields identical results to the unconvoluted calculation.

Again the experimental result for the two different extraction voltages is compared with the simulation. The scattering plane remains essentially uninfluenced, since here the momentum resolution has only minor effects. In the perpendicular plane, however, the experimental out-of-plane maxima at 90°/270° remain unchanged, whereas the simulation predicts a reduction by 30% in peak height. For an extraction of 20 V the simulation is about a factor of 2 too small compared to the experimental data. Hence, the features in the measured data cannot be explained solely by the experimental resolution. Here again, the insensitivity of the experimental FDCS to the extraction voltage suggests that the overall resolution is significantly better than the one used in the simulation. Therefore, even the simulation for 20 V probably overestimates the peak heights in the perpendicular plane.

The question whether the enhancement of the cross section is of physical nature and not merely a result of experi-

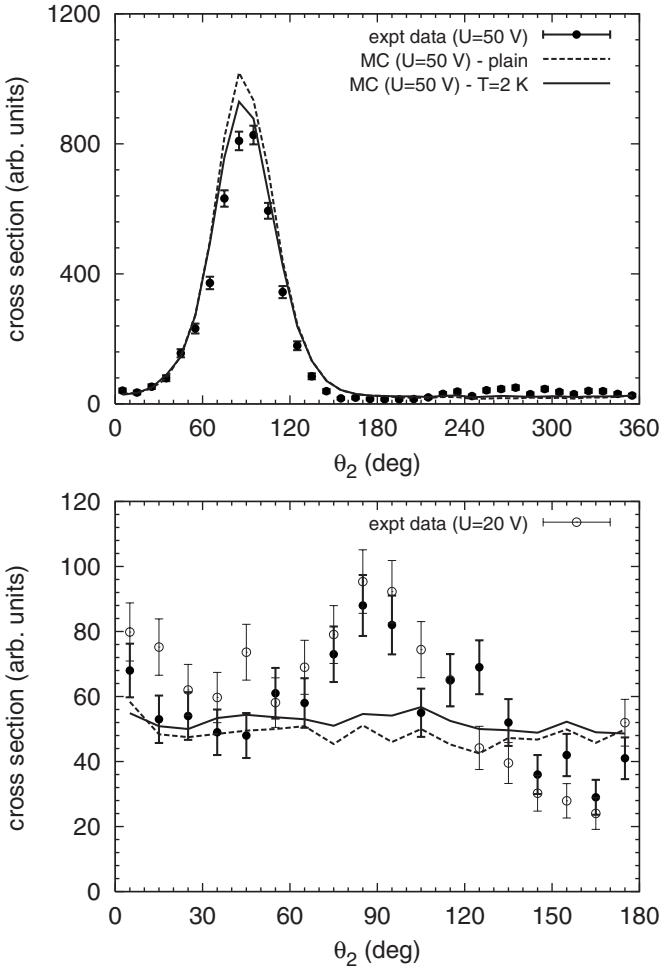

FIG. 8. Differential cross sections for single ionization of helium by 100 MeV C^{6+} in the scattering plane (top) and the plane perpendicular to the scattering plane (bottom). The energy of the ejected electron was integrated over a range $E_e=3-50$ eV and the momentum transfer $q_\perp=(1.5\pm0.5)$ a.u. were chosen. The displayed events are integrated within ±10° of the respective cutting planes.

mental uncertainties can be further studied at larger momentum transfers. Here, larger recoil-ion momenta are involved, such that the relative effects from the momentum resolution are less important than at smaller momentum transfers. Unfortunately, the cross sections drop rapidly with increasing momentum transfer, so that the FDCS extracted from the data are afflicted with larger error bars than at smaller q. Therefore, for a larger momentum transfer of $|\mathbf{q}|=(1.5\pm0.5)$ a.u. FDCS integrated over a wider range of ejected electron energies ($E=3-50$ eV) were generated. Again, we focus on electron emission in the scattering plane and the perpendicular plane (Fig. 8). We improve the statistics in the perpendicular plane by taking advantage of the required (model-independent) symmetry about 180° and added the counts for the angular ranges 0 to 180° and 360° to 180°. The measured and simulated cross sections are normalized to the same total cross section in order to have a comparison in both shape and magnitude. In the scattering plane we obtain a similar result as in the FDCS at smaller momentum transfer for a simulated resolution of 1 mm beam size and 2 K target temperature. The binary peak is well reproduced, whereas the recoil peak remains underestimated by the simulation. In the perpendicular plane, the peak at 90°, which was present in the simulation at the smaller momentum transfer of 0.75 a.u., has essentially disappeared at larger q. Since the out-of-plane structure obtained in the simulation exclusively stems from the recoil resolution, this is expected since for $|\mathbf{q}|=1.5$ a.u. the resolution should have less effect. However, in the experimental data an enhancement at 90° persists for both analyzed extraction voltages. In the simulation a peak structure is only obtained for temperatures larger than 6 K and the shape of the data cannot be reproduced with any temperature. This strongly suggests that the enhancement in the cross section perpendicular to the scattering plane to a significant part results from a true physical effect since all possible effects of the experimental resolution have been correctly simulated (or, in fact, overestimated). In fact, at momentum transfers larger than approximately 1 a.u. the convoluted ($T=2$ K) and unconvoluted simulations differ by less than 10% in the perpendicular plane and thus here the shape of the FDCS is dominated by the true physical shape.

V. EFFECTS OF THE EXPERIMENTAL RESOLUTION IN $(e,2e)$ BY 1 keV ELECTRONS

In a recent article [5], FDCS for single ionization of helium by 1 keV electron impact, using a refined design of the reaction microscope, were presented. A major improvement over the original design could be achieved by guiding the projectile beam exactly parallel to the electric and magnetic fields. A multihit electron detector with a hole in the middle, to allow the undeflected projectile beam to pass through the detector, was centered on the projectile beam axis. As a result, the scattered projectile electrons can be directly measured and momentum analyzed, in contrast to the experiments for the ionic projectiles. Therefore, the momentum information of the recoiling ion is not needed in order to fix the collision kinematics. It was nevertheless measured, which enabled us to directly determine the overall experimental resolution by using momentum conservation.

As the detection of the fast scattered projectile electron represents a novelty of our experiment, a brief description of the analysis of its momentum is given. For the final state particles, the z component of the momentum is purely deduced from the time-of-flight, whereas the detector position and the time of flight is needed to deduce the transverse x and y components. For collisions in which the scattered projectile loses only a small fraction of its initial energy and momentum, the longitudinal momentum cannot be directly measured due to the limitations of the timing resolution of the detection system. Instead, the longitudinal momentum transfer is obtained from the energy transfer to the target through the relation $q_z=(E_e+V_{\text{ion}})/v_P$. The transverse momentum components of the scattered projectile are easily measured with the same resolution as for any electron at lower energy.

For the electrons the resolution can be estimated from the time and position resolution, which in turn is given by the temporal width of the pulsed projectile beam (1.5 ns) and its

beam focus (diameter: 1 mm), determining the size of the interaction volume. For all electrons the estimated uncertainty in the magnitude of the transverse electron component $\mathbf{k}_\perp$ does not exceed $\Delta|\mathbf{k}_\perp|=0.1$ a.u. The resolution for the azimuthal angle $\varphi=\arctan(k_x/k_y)$ is less than 10°. The experimental resolution in the $(e,2e)$ reaction microscope experiment can be checked by calculating the sum of all final state momenta in the respective x and y direction for each triple coincidence event. The width of the sum-momentum reflects the overall resolution of the two outgoing electrons and the recoil ion. A Gaussian fit yields an overall resolution of $\Delta p_{\mathrm{sum},x}=0.4$ a.u. and $\Delta p_{\mathrm{sum},y}=0.5$ a.u. These directly measured resolutions actually imply, that the target temperature is considerably smaller than 2 K in the $(e,2e)$ experiment. Since the design and operating parameters of the jet were essentially identical to the one used for the ion-impact experiments, there too the actual temperature is probably closer to the theoretical value of 1 K than to the upper limit of 2 K used in the simulation.

In order to study the effect of the limited resolution of the recoil momentum, the FDCS was extracted using two different ways of determining the momentum transfer: Either from the scattered projectile momentum $\mathbf{q}=\mathbf{p}_0-\mathbf{p}_1$ [as published in Ref. [5], $E_e=(6.5\pm1)$ eV and $|\mathbf{q}|=(0.75\pm0.2)$ a.u.], or from the target fragments $\mathbf{q}=\mathbf{k}+\mathbf{p}$. In the former method, the overall resolution is about a factor of 3 better than in the latter and the simulation then yields practically identical results to the unconvoluted calculation. The kinematics where chosen just as in the C^{6+}-ion impact experiment.

The comparison of the cross sections, which have been relatively normalized to each other, is shown in Fig. 9, where we compare the FDCS in the scattering plane and in the plane perpendicular to the momentum transfer direction. In the plane perpendicular to $\mathbf{q}$ enhanced emission out of the scattering plane becomes visible as distinct maxima at around 90° and 270° as for the C^{6+} ion impact data. For electron collisions, the out-of-plane emission relative to the coplanar cross section is by a factor 2 weaker than that observed for ion impact. Most importantly, the results for the electron-electron coincidences are practically identical to those obtained from the ejected electron–recoil-ion coincidences. Since for the resolution achieved in the former method the simulation does not yield any peak structure at all in the perpendicular plane, they are practically entirely due to real physical effects. This means that even the electron–recoil-ion coincidences yield quantitatively accurate results which are not significantly affected by the experimental resolution. An extensive discussion in comparison with several advanced theoretical models will be subject to a forthcoming publication.

It should be noted that the overall resolution for the electron–recoil-ion coincidences is worse than for C^{6+} impact at 20 V extraction. Since the electron–recoil-ion coincidence data for electron impact data are not significantly affected by the resolution (see above), this must be the case to an even larger extent for the better resolution achieved for the ionic projectiles. The comparison to the electron impact data therefore shows that for C^{6+} impact the contribution of the resolution to the out-of-plane peak structure at $q=0.75$ a.u. must be significantly less than 50%.

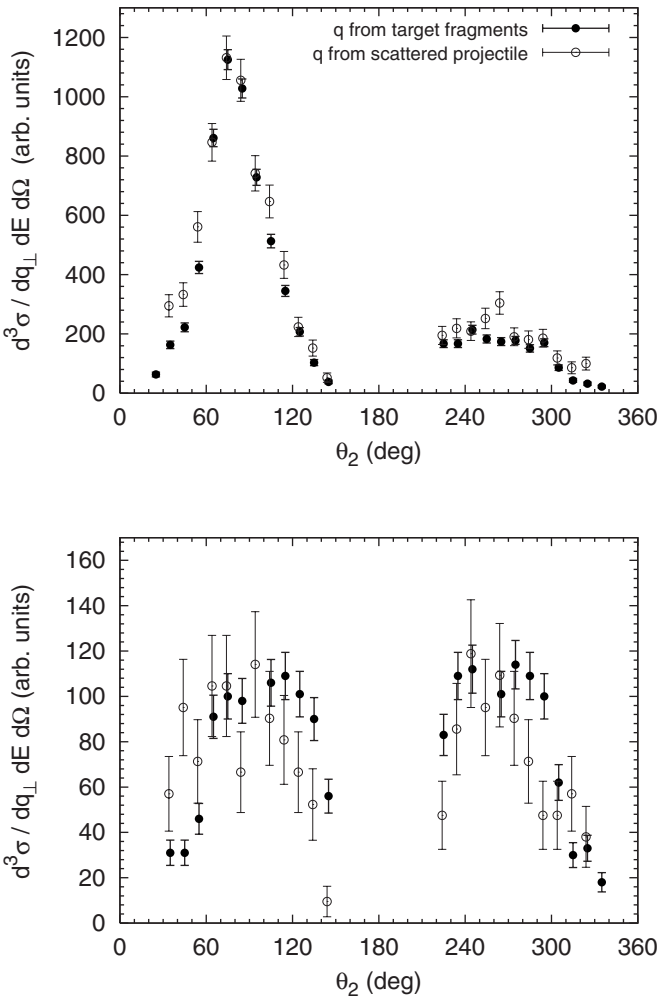

FIG. 9. Fully differential cross sections for single ionization of helium by 1 keV electrons in the scattering plane (top) and the plane perpendicular to the scattering plane (bottom). Solid circles: Data analyzed using the momentum analyzed ejected electron and the recoil ion. Empty circles: Data obtained from the momentum analyzed scattered projectile and ejected electron (from Ref. [5]).

VI. SUMMARY AND CONCLUSIONS

In this article we presented a thorough analysis of all known instrumental effects on multiply differential cross sections obtained with the reaction microscope for three collision systems, single ionization of helium by 100 MeV/C^{6+}, 3.6 MeV Au^{53+}, and 1 keV electron impact by means of a Monte Carlo simulation based on quantum theory. Generating an event file, simulating a data file obtained in the experiment according to the fully differential probability distribution predicted by quantum-mechanical models, allows one to fully incorporate the instrumental function in the comparison of theoretical and experimental cross sections. A conventional convolution of theory with the complete experimental resolution is extremely difficult and time consuming because of the multidimensionality of the three-body reaction. In particular experimental data collected with modern imaging techniques (reaction microscopes) covering a large part of the momentum phase space benefits from the Monte Carlo simulation technique.

The achievable momentum resolution of the reaction microscope using supersonic target jets is dominated by the momentum resolution of the recoiling ion, where in addition to the thermal motion in the target beam, the size of the overlap region between projectile and target beam considerably contributes to the resolution. By analyzing the distribution of the sum momenta of the target fragments, information on an upper limit of the parameters determining the actual momentum resolution in the different experiments is obtained. The simulation of the cross sections, using these upper limits (1 mm $\times$ 1 mm projectile beam diameter, 2 K target temperature), reveals a significant influence of the resolution on the differential data. The simulated results only partly reproduce the experimental cross sections, however, overall large discrepancies to the experimental data are found. For Au^{53+} collisions the shape of the experimental data cannot be reproduced under any circumstance, in particular in the FDCS the dominant peak for 0° electron emission in direction of the incoming projectile remains unexplained.

For single ionization by 100 MeV/u C^{6+} projectiles, where because of the small perturbation the collision dynamics is considered to be less complex than for the Au^{53+} projectiles, we find that the inclusion of instrumental effects in our simulation based on the FBA can lead to out-of-plane structures in the noncoplanar scattering geometry at 90° and 270°, where strong disagreement with nonconvoluted theory was reported. This discrepancy is significantly reduced by inclusion of the experimental uncertainties but still cannot be completely explained, especially for data at lower extraction voltage, where a factor of 2 enhancement of the experimental data compared to the simulation persists. In a further analysis of the data, especially at large momentum transfer, where the resolution shows essentially no effect, some discrepancy in the transverse plane remains. This implies that the out-of-plane features are at least partly due to a real physical effect. In fact, at momentum transfers larger than approximately 1 a.u. the out-of-plane structures are predominantly due to such effects. In contrast, for smaller momentum transfers it is presently only clear that the contribution from the resolution to the peak structure in the perpendicular plane is less than 50%. In order to determine these contributions more accurately new experiments with an even more tightly collimated beam and smaller extraction voltage are necessary. Within the last five years a completely new beamline with superior vacuum conditions and excellent beam optics was built at the Max-Planck-Institut für Kernphysik (MPIK) in Heidelberg. Many parameters influencing the resolution, like the pulse structure, the diameter and divergence of the beam delivered by the MPIK Tandem accelerator facility, can now be better controlled and optimized. With the resultant improved experimental resolution it will be possible to obtain more definite quantitative results on the out-of-plane structures even at small momentum transfers.

The collision systems of our present study represent simple and fundamental dynamical few-body systems, where theoretical models are increasingly successful in describing the underlying quantum dynamics. Modern imaging techniques provide powerful tools to experimentally explore such systems in very great detail. As instrumental effects cannot be avoided, their consideration in the comparison between theory and experimental data is vital, in order to obtain accurate results from the theoretical models and, thus, to advance our understanding of such systems. The present study demonstrates that event generators provide a reliable and extremely powerful pathway for benchmarking calculations against multiply differential experimental data where unavoidable instrumental image functions always influence the measured data.

[1] H. Ehrhardt *et al.*, Phys. Rev. Lett. **22**, 89 (1969).
[2] E. C. Beaty, K. H. Hesselbacher, S. P. Hong, and J. H. Moore, Phys. Rev. A **17**, 1592 (1978).
[3] T. Rosel, J. Roder, L. Frost, K. Jung, H. Ehrhardt, S. Jones, and D. H. Madison, Phys. Rev. A **46**, 2539 (1992).
[4] A. J. Murray and F. H. Read, Phys. Rev. Lett. **69**, 2912 (1992).
[5] M. Durr, C. Dimopoulou, B. Najjari A. Dorn, and J. Ullrich, Phys. Rev. Lett. **96**, 243202 (2006).
[6] N. V. Maydanyuk, A. Hasan, M. Foster, B. Tooke, E. Nanni, D. H. Madison, and M. Schulz, Phys. Rev. Lett. **94**, 243201 (2005).
[7] R. Moshammer *et al.*, Nucl. Instrum. Methods Phys. Res. B **108**, 425 (1996).
[8] M. Schulz *et al.*, J. Phys. B **34**, L305 (2001).
[9] M. Schulz *et al.*, Nature (London) **422**, 48 (2003).
[10] D. Madison *et al.*, J. Phys. B **35**, 3297 (2002).
[11] A. B. Voitkiv, B. Najjari, and J. Ullrich, J. Phys. B **36**, 2591 (2003).
[12] M. Durr *et al.*, J. Phys. B **39**, 4097 (2006).
[13] R. W. v. Boeyen *et al.*, Phys. Rev. A **73**, 032703 (2006).
[14] R. Moshammer, A. Perumal, M. Schulz, V. D. Rodriguez, H. Kollmus, R. Mann, S. Hagmann, and J. Ullrich, Phys. Rev. Lett. **87**, 223201 (2001).
[15] M. Schulz *et al.*, J. Phys. B **35**, L161 (2002).
[16] D. Fischer *et al.*, J. Phys. B **36**, 3555 (2003).
[17] D. H. Madison, D. Fischer, M. Foster, M. Schulz, R. Moshammer, S. Jones, and J. Ullrich, Phys. Rev. Lett. **91**, 253201 (2003).
[18] M. Foster, J. L. Peacher, M. Schulz, D. H. Madison, Z. Chen, and H. R. J. Walters, Phys. Rev. Lett. **97**, 093202 (2006).
[19] R. E. Olson and J. Fiol, Phys. Rev. Lett. **95**, 263203 (2005).
[20] S. Otranto, R. E. Olson, and J. Fiol, J. Phys. B **39**, L175 (2006).
[21] J. Fiol, S. Otranto, and R. E. Olson, J. Phys. B **39**, L285 (2006).
[22] J. Fiol and R. E. Olson, J. Phys. B **37**, 3947 (2004).
[23] M. Foster *et al.*, J. Phys. B **37**, 3797 (2004).
[24] P. D. Fainstein and L. Gulyas, J. Phys. B **38**, 317 (2005).
[25] R. T. Pedlow, S. F. C. O'Rourke, and D. S. F. Crothers, Phys. Rev. A **72**, 062719 (2005).
[26] J. Ullrich *et al.*, J. Phys. B **22**, 627 (1989).
[27] R. Dorner, J. Ullrich, R. E. Olson, O. Jagutzki, and H.

Schmidt-Bocking, Phys. Rev. A **47**, 3845 (1993).
[28] J. Ullrich *et al.*, J. Phys. B **30**, 2917 (1997).
[29] J. Ullrich *et al.*, Rep. Prog. Phys. **66**, 1463 (2003).
[30] J. Ullrich and V. P. Shevelko, *Many-Particle Quantum Dynamics in Atomic and Molecular Fragmentation* (Springer, Berlin, 2003).
[31] W. C. Wiley and I. H. Mclaren, Rev. Sci. Instrum. **26**, 1150 (1955).
[32] J. P. Toennies and K. Winkelmann, J. Chem. Phys. **66**, 3965 (1977).
[33] V. L. B. de Jesus *et al.*, J. Electron Spectrosc. Relat. Phenom. **141**, 127 (2004).
[34] R. Moshammer *et al.*, Phys. Rev. Lett. **73**, 3371 (1994).
[35] A. B. Voitkiv and B. Najjari, J. Phys. B **37**, 4831 (2004).
[36] H. Berg *et al.*, J. Phys. B **25**, 3655 (1992).